Journal of Molecular Catalysis A: Chemical 353–354 (2012) 22–28

Contents lists available at SciVerse ScienceDirect

Journal of Molecular Catalysis A: Chemical

journal homepage: www.elsevier.com/locate/molcata

Synthesis and photocatalytic performance of the efficient visible light photocatalyst Ag–AgCl/$BiVO_4$

Zhijun Zhou, Mingce Long*, Weimin Cai, Jun Cai

School of Environmental Science and Engineering, Shanghai Jiao Tong University, Dongchuan Road 800, Shanghai 200240, China

ARTICLE INFO

Article history:
Received 11 September 2011
Received in revised form 31 October 2011
Accepted 31 October 2011
Available online 9 November 2011

Keywords:
Visible light
Photocatalyst
Ag nanoparticles
AgCl
$BiVO_4$

ABSTRACT

A visible-light responsive photocatalyst consisting of Ag–AgCl composite dispersed over $BiVO_4$ (Ag–AgCl/$BiVO_4$) was synthesized via a photolysis and calcination method. The effects of synthetic conditions such as Ag contents, molar ratios of chlorine to silver and calcination temperatures have been discussed. The coupling Ag–AgCl composite structure, which is necessary for the high photoactivity, comes into being by partially converting Ag nanoclusters into AgCl during heat treatment. The discoloration efficiency of methyl orange over the as-prepared Ag–AgCl/$BiVO_4$ was more than 90% after 120 min under visible light irradiation. In the Ag–AgCl/$BiVO_4$ system, the coupled processes of excitation from valence band of AgCl to the sensitizer Ag nanoparticles and the surface plasmonic resonance of Ag nanoparticles mainly contributed to its high activity. In addition, the presence of $BiVO_4$ changed the hole transfer process, and $O_2^{-\bullet}$ became to be the solely main active specie in the degradation reaction. The photocatalytic activity can be further improved by the addition of hole scavengers.

1. Introduction

Heterogeneous photocatalysis has been regarded not only as a cost-effective technology for the reduction and elimination of persistent toxic organic pollutants, but also as a promising alternative for solar energy utilization [1–3]. However, in practical applications it has been limited for the low utilization of solar energy in both optical absorption and energy conversion. Therefore, the development of efficient photocatalysts responsive in a wide range of solar spectrum has played an important role in this field. Two approaches have been developed to exploit desirable photocatalysts: the first one involves doping or modifying UV active semiconductor oxides (such as TiO_2) to turn them into visible light responsive photocatalysts [4–6]; the second is to design novel complex compounds or fabricate composites [7,8], such as $PbBi_2Nb_{1.9}W_{0.1}O_9/CaFe_2O_4$ [9], graphene oxide enwrapped Ag/AgX (X = Br, Cl) [10], and so on. At present, solar energy photocatalytic conversion for environment and energy applications still requires more efficient visible light driven photocatalysts.

The surface plasmonic resonance (SPR) nanostructures, which are originated from the coupling collective oscillations of surface electrons with the incident photons [11,12], have already gained considerable attention in many fields, including nanoscale optical devices [13], enhanced spectroscopy [14], solar cells [15], and so on [16]. Recently, further applications have been explored in the field of photocatalysis for organic decomposition [12,17,18], CO oxidation [19] and water splitting [16] under visible light irradiation. It is well known that noble metal nanoparticles (NPs) show strong UV–vis absorption due to their SPR nanostructures. Moreover, AgCl, AgBr and AgI [20,21], known as widely applied photosensitive materials, were firstly reported as photocatalysts for water splitting in 1999. Inspired by the photosensitive properties and the SPR effect of Ag NPs, high efficient plasmonic photocatalysts Ag/AgX have been developed and aroused broad interesting and concerning [1,17,22–26]. Wang et al. synthesized AgCl particles with silver NPs deposited on their surface (Ag@AgCl), by first treating Ag_2MoO_4 with HCl in an ion-exchange reaction to form AgCl powder and then irradiating AgCl to reduce some Ag^+ ions [17]. Hu et al. prepared Ag–AgI/Al_2O_3 via a photocatalytic reduction method [1]. Yu et al. obtained visible-light-driven plasmonic photocatalyst Ag/AgCl/TiO_2 nanotube arrays by first depositing AgCl nanoparticles (NPs) into the self-organized TiO_2 NTs, and then reducing partial Ag^+ ions to Ag^0 species upon irradiation [26]. Although there are a few approaches to fabricate highly activity Ag/AgX structures, effects of synthetic conditions on the formation and the components of the active Ag/AgX are still not clear. According to the results of photocurrent measurements, radical analysis and photocatalytic activity tests, the $O_2^{-\bullet}$ and holes have been regarded as the main active species. However, it is unknown which substance, plasmon-excited Ag-NPs [1] or photosensitized AgX [17], generates these active species. In fact, exclusive Ag or AgX shows very low photocatalytic activity.

* Corresponding author. Tel.: +86 21 54747354; fax: +86 21 54740825.
E-mail address: long_mc@sjtu.edu.cn (M.C. Long).

1381-1169/$ – see front matter © 2011 Elsevier B.V. All rights reserved.
doi:10.1016/j.molcata.2011.10.025

$BiVO_4$ is a kind of visible light driven photocatalysts with a band gap of 2.4 eV for the monoclinic scheelite structure. The $BiVO_4$ microparticles can be facilely obtained via a homogeneous precipitation method [27], and applied in water purification due to its good precipitation performance [9]. However, its activity is restricted by large particles and serious recombination of charge carriers. Herein, $BiVO_4$ was employed as a support for the highly active Ag–AgCl structure, and a new Ag–AgCl/$BiVO_4$ composite photocatalyst was prepared via a facile photolysis and calcination method. The prepared samples showed high visible light photocatalytic activity for the photocatalytic degradation of methyl orange (MO) aqueous solution. Furthermore, the effect of source materials and the synthetic conditions have been studied, and a charge transfer mechanism has been discussed.

2. Experimental

2.1. Materials

Silver nitrate ($AgNO_3$), ammonia chloride (NH_4Cl), bismuth nitrate ($Bi(NO_3)_3{\cdot}5H_2O$), ammonium metavanadate (NH_4VO_3) and methyl orange (MO) were procured from Sinopharm Chemical Reagent Co., Ltd. Ammonia was obtained from Pinghu Chemical Reagent Factory. All chemicals are of analytical-grade and used without further purification.

2.2. Sample preparation

$BiVO_4$ was synthesized in aqueous media via a homogenous precipitation method with $Bi(NO_3)_3$ and NH_4VO_3 [27]. $AgNO_3$ was employed as the source of silver and dissolved in the aqueous ammonia to obtain a $[Ag(NH_3)_2]^+$ solution with a concentration of 0.373 mol/L. NH_4Cl was selected as the source of chlorine. In a typical synthesis procedure, 1 g $BiVO_4$ powder was dispersed in 8 ml deionized water, and then 2 ml NH_4Cl solution (0.373 mol/L) and 1 ml of $[Ag(NH_3)]^+$ solution were added in turn. After being stirred at room temperature for 6 h, the mixture solution, accompanying with continuous stirring, was irradiated with 1000 W xenon lamp for 1 hour. Finally the resulting powder was dried completely at 60 °C overnight (the dried sample designated as S-D). The sample S-D was calcined at 500 °C for 3 h to obtain a light yellow powder, referred as Ag–AgCl/$BiVO_4$ for convenience. A control sample S-W was prepared by washing S-D with a large amount of water, drying and calcining at 500 °C for 3 h. The influence of temperatures (T), amounts of silver (Ag%) and molar ratios of chlorine and silver (Cl/Ag) has been investigated.

2.3. Photocatalytic activity measurements

The optical system for photocatalytic reaction consists of a 1000 W xenon lamp operating at an output power of 700 W and a cutoff filter with larger than 90% transmission ($\lambda > 400$ nm). The batch reactor is a 100 ml glass container with circulating cooling water outside in a homemade dark box, and the light illuminated from the upside with a distance of 1.2 m away from the reactor surface. In a typical photocatalytic activity test, 0.05 g prepared catalyst was added into a 50 ml methyl orange (MO) solution (10 mg L^{-1}), then the dispersion was kept in dark for 10 min to obtain the equilibrium adsorption state. During the irradiation, the temperature of the solution was maintained by cooling water. Under continuous stirring, samples were taken at half-hourly intervals, filtered and then analyzed by a UNICO UV-2102 spectrometer at 464 nm. The leached metal ions were measured by an inductive coupled plasma (ICP) spectrometer (Thermo, iCAP 6000 Radial).

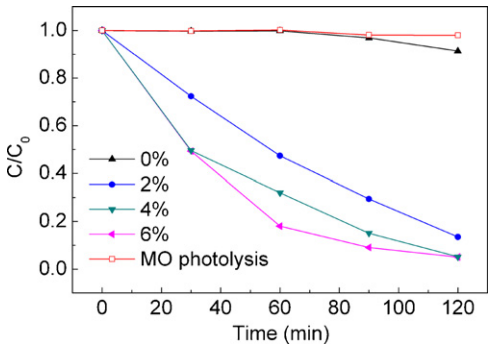

Fig. 1. The decrease of MO as a function of irradiation time over photocatalysts with various Ag content (Cl/Ag = 2; T = 500 °C, catalyst load = 1 g L^{-1}) or without photocatalyst (initial concentration of MO = 10 mg L^{-1}).

2.4. Material characterization

The crystal phase of samples were characterized by powder X-ray diffraction (XRD, D/max-2200/PC, Rigaku Corporation, Japan), operating at 40 kV and 30 mA, where λ = 0.15418 nm for the Cu K_α line. Diffuse reflectance spectra (DRS) were obtained on a UV–Vis spectrophotometer (TU-1901, China) equipped with a diffuse reflectance accessory, and the reflectance was converted to $F(R_\infty)$ values according to the Kubelka–Munk method. The chemical states of elements were measured by a RBD upgraded PHI-5000C ESCA system (Perkin Elmer, USA), and the shift of the binding energy due to relative surface charging was corrected using the C 1s level at 284.6 eV as an internal standard. Differential scanning calorimeter (DSC) and thermogravimetric analysis (TGA) were carried out to track the changes during the heat treatment by a simultaneous thermal analyzer (NETZSCH STA 449 F3 Jupiter). The nanometric structure and the morphology of the catalysts were observed by transmission electron microscope (TEM, JEM-100CX, JEOL, Japan) and a field emission scanning electron microscope (FE-SEM, FEI SIRION 200).

3. Results and discussion

3.1. Effect of Ag content

As shown in Fig. 1, the photolysis of MO under visible light is negligible. Without modification, the activity of pure $BiVO_4$ is weak, resulting in less than 10% of MO reduction after 120 min irradiation. It can be attributed to large particle sizes of the synthesized $BiVO_4$ and the poor migration of photogenrated carriers over $BiVO_4$ [9]. However, by importing silver compounds over the surface of $BiVO_4$ particles with only a very small amount, the photocatalytic activity has been enhanced dramatically. It indicates that the presence of plasmonic Ag–AgCl components great contributes to the MO reduction and is crucial for the high photocatalytic activity. Although the sample with Ag content of 6% showed a little higher activity, the sample of 4% Ag content was employed for the following investigations due to the consideration of its lower cost.

3.2. Effect of the ratio of NH_4Cl to Ag

NH_4Cl is selected as the source of chloride for the consideration of not importing foreign cations after calcinations. In Fig. 2, only in the presence of $[Ag(NH_3)]^+$ without NH_4Cl, the as-prepared catalyst shows an even lower activity than that of pure $BiVO_4$, with nearly no reduction of MO observed. According to the reports by Kohtani et al. [28,29], Ag-loaded $BiVO_4$ exhibits enhanced photocatalytic activity due to the synergetic effects of the specific adsorption by silver oxides and an increase in the reaction rates by metallic Ag

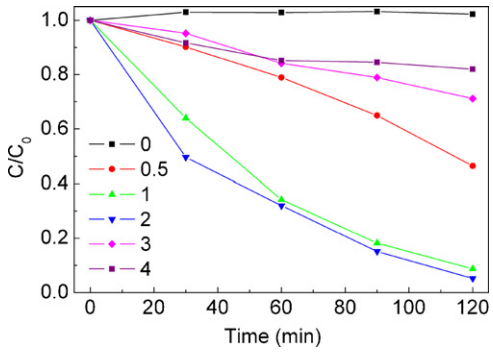

Fig. 2. The decrease of MO as a function of irradiation time over photocatalysts with various molecular ratio of NH_4Cl to Ag (Ag% = 4 wt%; T = 500 °C, catalyst load = 1 g L^{-1}, initial concentration of MO = 10 mg L^{-1}).

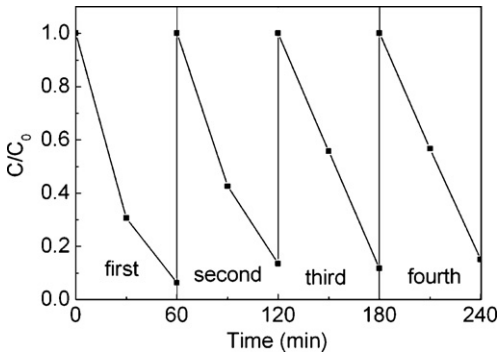

Fig. 4. Cycling runs for the photodegradation of MO in the presence of Ag–AgCl/$BiVO_4$ under visible irradiation (catalyst load = 2 g L^{-1}; initial concentration of MO = 10 mg L^{-1}).

modification. Although a similar Ag loaded $BiVO_4$ (Ag–$BiVO_4$) was obtained without adding NH_4Cl, our method is quite different from the impregnation method by them. In the impregnation method the Ag or silver oxides were formed homogenously over the surface of $BiVO_4$. However in our method, dryness by irradiating promoted the processes of photolysis of silver compounds and agglomeration of Ag particles. Due to the higher mass ratio of Ag (4 wt%), a higher coverage of the inactive Ag or silver oxides blocks the excitation of $BiVO_4$, resulting in the low active catalyst.

It has been reported that the surface plasmonic resonance could induce efficient photocatalytic activity. With the addition of NH_4Cl in the precursor solution and calcinations at 500 °C, Ag–AgCl heterojunction structure is formed, so as to make inside silver free from oxidation during calcination. In consideration of the mass loss of chloride during the calcination process, an overdose of NH_4Cl is necessary for the formation of optimized Ag–AgCl components. However, too much addition of NH_4Cl during the synthetic process would also result in a significant decrease of the activity, because in that case, all the silver would be chemical combined with chloride and transforms into the exclusive AgCl, which greatly reduces the efficient plasmonic photocatalytic effect.

3.3. *Effect of calcination temperature*

The effect of calcination temperatures has been studied in the present research. According to Fig. 3, calcinations are necessary for high efficient photocatalysts. The dried sample (S-D), which has not been calcined, shows a slight dark yellow color and low activity for MO reduction (only 36.3% MO reduced in 120 min). However, its activity is obviously higher than that of the pure $BiVO_4$ and Ag–$BiVO_4$. It suggests that a better efficient Ag–AgCl heterojunction structure has been preliminarily formed. Under calcination at elevated temperatures, the adsorbed chlorides chemically bond with silver and then form AgCl over the surface of Ag. According to the standard Gibbs free energy (ΔG_f^θ), AgCl is −26.244 kJ/mol, which is lower than that of Ag_2O or AgO, whose ΔG_f^θ is −2.68 or −3.40 kJ/mol, respectively [30]. Therefore AgCl is thermodynamically more stable and easier to generate than Ag_2O and AgO. Moreover, increasing temperature favors the conversion of AgO or Ag_2O into AgCl due to the positive entropy of this reaction. Therefore calcination promotes the Ag or silver oxides in the dried sample transforming into AgCl. The presence of the adsorbed chloride in the dried sample (S-D) for the formation of AgCl in the subsequent calcination can be confirmed by the poorer activity of the washed and calcined sample (S-W). The MO reduction over this synthesized catalyst is decreased to 37.6%, close to the activity of sample S-D but much lower than that of Ag–AgCl/$BiVO_4$. Above results indicate that: (1) there is some AgCl formed during the dryness process and (2) during calcinations, chloride become decomposed and combined with silver to form AgCl, which is important to enhance photoactivity. On the other hand, the formation of AgCl over the surface of Ag particles can serve as a blocker to slow down the further conversion of inside Ag when the temperature is not too high and chloride not too much. The fabricated Ag–AgCl structure has been confirmed having an efficient photocatalytic activity due to the coupling effect of surface plasmonic resonance [17,25]. From Fig. 3, the sample calcined at 500 °C has the highest activity and more than 90% MO can be reduced after 120 min irradiation. This sample, in which the Ag content was 4%, the molar ratio of NH_4Cl to Ag was 2 and the treatment temperature was 500 °C, is assigned as Ag–AgCl/$BiVO_4$.

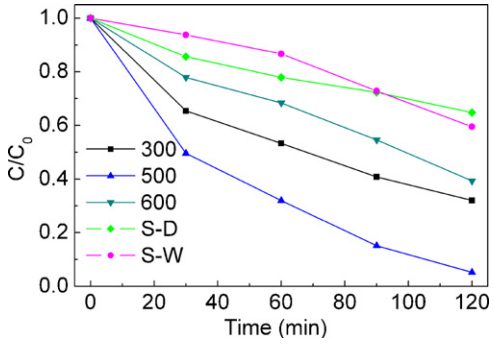

Fig. 3. The decrease of MO as a function of irradiation time over photocatalysts without calcinations (S-D) or calcined at 300, 400 or 500 °C and the sample S-W which calcined at 500 °C (Ag% = 4 wt%; Cl/Ag = 2, catalyst load = 1 g L^{-1}, initial concentration of MO = 10 mg L^{-1}).

The stability of this catalyst has been determined by leached metal ion measurements and recycled tests. After 2 h photodegradation, the solution was filtered by a G5 core funnel, and the metal ions in the solution were measured by an ICP spectrometer. Results showed that the metal ions of Bi, Ag and V are undetectable in the solution. The photocatalyst Ag–AgCl/$BiVO_4$ is also stable under repeated application, as shown in Fig. 4. After four successive cycles of degradation tests under visible irradiation, the activity did not obviously decrease. The colors of the solutions before and after the photocatalytic reaction over Ag–AgCl/$BiVO_4$ are shown in Fig. 5 (For interpretation of the references to color in text, the reader is referred to the web version of this article.). The solution almost became clear after the 5 min precipitation, and the original orange color has disappeared. The slightly yellow color of the final solution whose pH value is 4.07 can be attributed to the reflectance of the bottom yellow catalysts. Therefore this new composite could be employed as an efficient visible light driven photocatalyst for water purification and can be easily separated by precipitation.

Fig. 5. Pictures of solutions of MO after 5 min precipitation: (A) before photocatalytic degradation and (B) after photocatalytic reaction (120 min) over Ag–AgCl/$BiVO_4$ (catalyst load = 1 g L^{-1}; initial concentration of MO = 10 mg L^{-1}).

3.4. Characterization

The color of synthesized samples offers further hints of their different components and structures. Both $BiVO_4$ and Ag–AgCl/$BiVO_4$ show yellow color with the latter one a little lighter, while Ag–$BiVO_4$ and S-D exhibit a dark yellow color. Their optical properties have been characterized by measuring the DRS spectra and their corresponding $F(R_\infty)$ values have been obtained according to the Kubelka–Munk method. The results are shown in Fig. 6, accompanying with their digital pictures. Compared with other powders, Ag–$BiVO_4$ is characterized with an obvious absorption at 600 nm, which is originated from silver oxide particles and mainly contributes to its dark yellow color (For interpretation of the references to color in text, the reader is referred to the web version of this article.). There is also a slight absorption peak at 295 nm, corresponding to the Ag^0 particles. This absorption also appears in the sample S-D, which has a stronger absorbance above the band edge absorption of

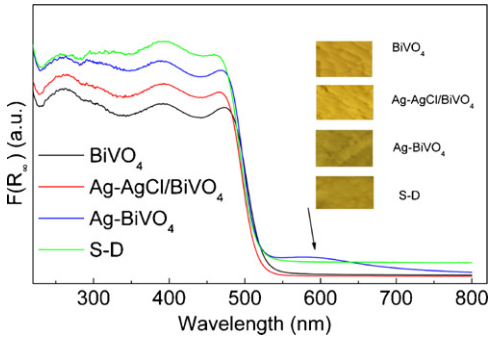

Fig. 6. Plot of Kubelka–Munk function *vs.* wavelength of light for $BiVO_4$, Ag–AgCl/$BiVO_4$, Ag–$BiVO_4$ and the sample S-D (insert is the digital pictures of corresponding powders).

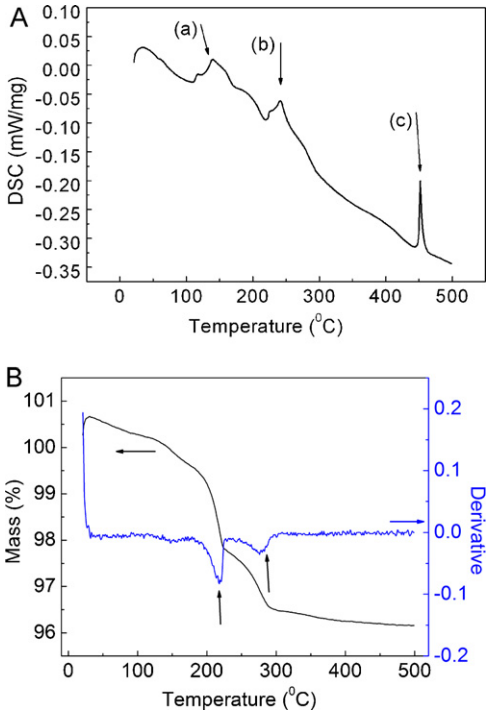

Fig. 7. DSC and TGA of the sample S-D (Ag% = 4 wt%; Cl/Ag = 2).

$BiVO_4$ but without any absorption peak as Ag–$BiVO_4$. This indicates that only Ag^0 contributes to the dark yellow color of the sample S-D. The peak at 295 nm is not so obvious for the sample Ag–AgCl/$BiVO_4$, which has almost the same spectrum as that of the pure $BiVO_4$. This can be attributed to that the Ag^0 particles have been shielded by the white AgCl compounds. Therefore Ag–AgCl/$BiVO_4$ appeared as the same light yellow color as $BiVO_4$.

The DTA and TGA curves have been measured to track the process of calcination, and the results are shown in Fig. 7. There are two obvious mass loss regions at 200 °C and 280 °C, and another smaller one at around 150 °C. The mass loss can be attributed to the evaporation of adsorbed water and ammonia, and the decomposition of NH_4Cl or Ag_2O compounds, all of those are endothermic. Another important endothermic peak at about 255 °C (in region a) corresponds to the reversible phase transition between monoclinic scheelite and tetragonal scheelite structure [31]. The curves also suggest that the recombination and formation of AgCl can be realized at a relatively low temperature (below 300 °C), because this reaction is an exothermic reaction and there is no obvious mass loss above 300 °C. The endothermic process at 450 °C without mass loss verifies the existence of AgCl because it corresponds to the melting point of AgCl. Heat treating catalysts above this temperature could favor homogeneous dispersion of AgCl–Ag over the support and an improved crystallinity of AgCl, both of which contribute to a higher catalytic activity.

From XRD patterns of catalysts (Fig. S1), such materials as monoclinic $BiVO_4$ with scheelite structure (JCPDS 14-0688) [9,31], cubic AgCl (JCPDS 31-1238), and a small amount of Ag (JCPDS 65-2871) [17,26], can be observed. To estimate the relative content of AgCl and Ag in various catalysts, the intensity has been compared at the strongest diffraction peaks at 32.3° for AgCl (2 0 0) plane and 38.1° for Ag (1 1 1) plane. The results are shown in Table 1, accompanying with the photocatalytic activity of catalysts. For the uncalcined (S-D) or the washed and calcined (S-W) sample, the ratio of intensity is 2.70 or 2.96, respectively, smaller than that of the sample Ag–AgCl/$BiVO_4$. This is the evidence for the conversion of Ag to AgCl during calcination. The lower intensity at 32.3° for S-W can

Table 1
The ratio of AgCl and Ag estimated from XRD intensity.

Catalysts	Intensity at 32.3° (AgCl)	Intensity at 38.1° (Ag)	Ratio of intensity (AgCl/Ag)	Activity[d](%)
Ag–AgCl/$BiVO_4$[a]	264.2	22.6	11.69	94.9
S-D[b]	222.4	82.4	2.70	36.3
S-W[c]	108.1	36.5	2.96	37.6

[a] Calcined at 500 °C.
[b] S-D: dried sample without calcinations.
[c] S-W: S-D was washed and calcined at 500 °C.
[d] The MO reduction after 120 min irradiation.

be attributed to the mass loss of chloride after washing process. Upon prolong irradiation, there are photodecomposed Ag particles formed in the dried sample, along with a little AgCl. However, the activity is low because AgCl is not enough for a well coupling Ag–AgCl structure. Calcination at 500 °C not only maintained the transformation of AgCl, but also promoted the melting of AgCl, so as to form a Ag–AgCl heterojunction structure with efficient photoactivity.

SEM and TEM images of the Ag–AgCl/$BiVO_4$ powder are displayed in Fig. 8. Anomalous $BiVO_4$ particles can be observed in the SEM image, together with several dots of Ag–AgCl deposited over the surface. TEM image revealed that the nanoparticles of silver and silver chloride with diameters in the range of 5–10 nm are deposited over the surface of $BiVO_4$ particle. However, the hetero components interface of Ag and AgCl cannot be verified in current analysis. XPS of Ag–AgCl/$BiVO_4$ has been measured to determine the chemical states of Ag. As shown in Fig. 9, two bands of silver binding energies at 367.5 and 373.4 eV can be ascribed to Ag $3d_{5/2}$ and Ag $3d_{3/2}$, respectively. To further deconvoluted the two bands, four peaks at 367.2, 368.4, 373.5 and 374.9 eV can be found, where the peaks at 367.2 and 373.5 eV are attributed to the Ag^+ of AgX, and those at 368.4 and 374.9 eV are ascribed to the metallic Ag^0 [10,25]. A rough area ratio of Ag^+ to Ag^0 is 4, indicating a larger proportion of AgCl in the sample. Moreover, the binding energies of Cl $2p_1$ and Cl $2p_3$ are approximately 197.9 eV and 199.5 eV, respectively, corresponding to the chemical bonded Cl with Ag [25]. Therefore, a Ag–AgCl composite is formed over the surface of $BiVO_4$.

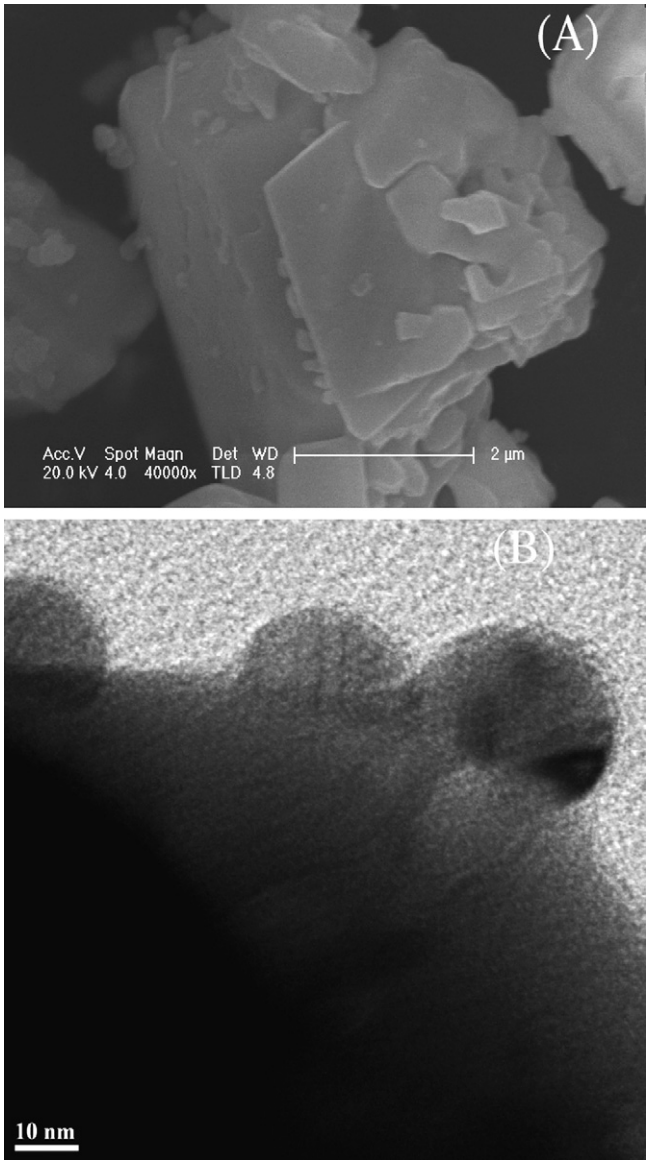

Fig. 8. Typical SEM (A) and TEM (B) images of Ag–AgCl/$BiVO_4$.

3.5. Mechanism discussion

Herein a new photocatalyst composite, Ag–AgCl dispersed over $BiVO_4$ has been fabricated by a facile method. In the precursor solution, there are ions of $[Ag(NH_3)_2]^+$, Cl^-, NO_3^-, OH^-, etc. $BiVO_4$ powder served as the support. Upon irradiation from Xe lamp, the silver compounds were photolyzed and produced elementary silver nanoclusters. It should be noticed that there are adsorbed chlorides dispersed over the surface of Ag or $BiVO_4$ in the dry sample (S-D). Then under heat treatment, chlorides were decomposed, recombined with Ag and transformed into AgCl over the surface of Ag particles. The previous irradiation is necessary for a high active catalyst, because a comparison test dried in dark can achieve only 54% MO reduction after 120 min irradiation. Moreover, a promoted photolysis test has been carried out at the presence of electron scavenger methanol upon irradiation. The as-prepared sample shows even better performance with more than 97% MO reduction in 120 min. This means that the presence of Ag nanoclusters is a prerequisite for the generation of a proper Ag–AgCl composite. To determine the role of ammonia, another comparison sample with $AgNO_3$ aqueous solution and diluted HCl as the precursors has been prepared. The decrease of MO over this comparison sample has been only 54.2% after 120 min irradiation. This can be understood by the fact that the formation of Ag nanoclusters can be accelerated by the presence of ammonia, because the reduction potential of $Ag(NH_3)_2^+$ ($E^\theta(Ag(NH_3)_2^+/Ag^0 + 2NH_3) = -2.2$ V) is more cathodic than silver ions ($E^\theta(Ag^+/Ag^0) = -1.8$ V) [32].

According to above analyses and reference results, the coupled Ag–AgCl with proper composition is necessary to achieve an efficient activity for organic degradation. To further explain the principle of photocatalytic process over the Ag–AgCl/$BiVO_4$ catalyst, several radical scavengers were employed in the photocatalytic degradation of MO, and the results are shown in Fig. 10. In the N_2 saturated solution, MO degradation over Ag–AgCl/$BiVO_4$ has been significantly suppressed. Moreover, the typical hydroxyl radical scavengers of isopropanol and methanol have little influence on the photocatalytic activity, indicating that $OH^\bullet$ in the bulk solution does not play a major role in the photodegradation system. This is consistent with the previous report [1]. However, it is surprising that the activity of Ag–AgCl/$BiVO_4$ is obviously improved by $NaHCO_3$, and MO degradation has been enhanced a little with the increase of $NaHCO_3$ concentration from 0.01 M to 0.1 M. It has been reported that the presence of $NaHCO_3$ inhibited the photodegradation of 2-chlorophenol over catalyst Ag–AgI/Al_2O_3 [1]. The suppressed effect of $NaHCO_3$ has also been confirmed using

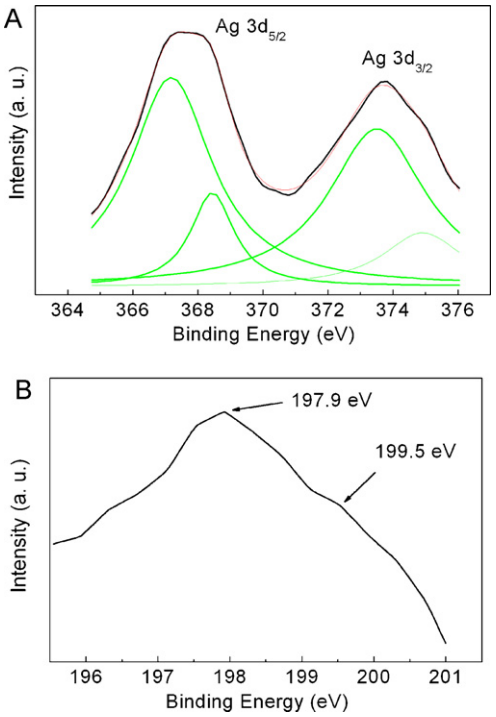

Fig. 9. XPS spectra of Ag 3d (A) and Cl 2p (B) of Ag–AgCl/$BiVO_4$.

another similar sample Ag–AgCl/SBA-15 (Fig. S2). This suggested that both $O_2^{-\bullet}$ radicals and holes are active species in the photocatalytic reaction with an inert support such as SBA-15 and Al_2O_3. As a matter of fact, because the point of zero charge of $BiVO_4$ is pH = 2.7 [33] and the acidic character is strong over the surface of $BiVO_4$, the basic species HCO_3^- could be prone to adsorb on the catalyst surface [34,35]. On the other hand, the holes in the valence band can preferentially react with the HCO_3^- anion having negative charge. Therefore HCO_3^- anions are typical scavenger for the adsorbed $OH^\bullet$ radical or holes [35,36]. The observed enhancement by $NaHCO_3$ for Ag–AgCl/$BiVO_4$ can be attributed to the promoted scavenging of holes and the improved separation of the photogenerated electrons and holes [36]. Photogenerated electrons are trapped by oxygen to form $O_2^{-\bullet}$, which is the mainly active species in the reaction with Ag–AgCl/$BiVO_4$. The important role of $O_2^{-\bullet}$ in this system has been further confirmed by a comparison test for phenol degradation in the presence of p-benzoquinone (Fig. S3). The distinct result of the effect of $NaHCO_3$ is ascribed to the photocatalyst support $BiVO_4$, which is different with the inert support SBA-15. The photoexcited processes over Ag–AgCl/$BiVO_4$ can be understood by the following suggested mechanism (Scheme 1). Under visible light irradiation,

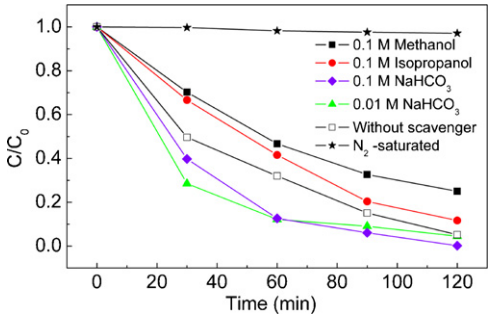

Fig. 10. The decrease of MO as a function of irradiation time in Ag–AgCl/$BiVO_4$ suspension under visible irradiation ($\lambda > 400$ nm) with or without scavengers, or in N_2-saturated solution (catalyst load = 1 g L^{-1}; initial concentration of MO = 10 mg L^{-1}).

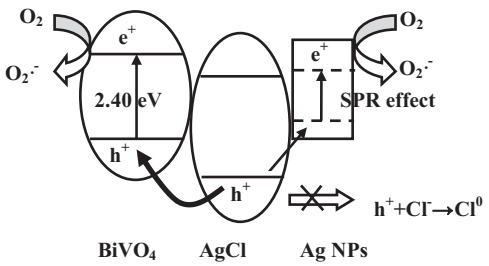

Scheme 1. Schematic diagram for the charge separation in the visible light irradiated Ag–AgCl/$BiVO_4$ system.

photogenerated electron–hole pairs are formed both in the Ag NPs sensitized AgCl and $BiVO_4$. The direct band gap and indirect band gap for AgCl are 5.6 eV and 3.25 eV, respectively. Therefore the excitation occurring over the coupled Ag–AgCl could not be originated from the band excitation of AgCl. Under illumination, the electrons in the valence band of AgCl can be excited to the electronic level of Ag NPs, which locates in the band gap of AgCl [37]. Simultaneously, electron excitation can occur by SPR effect in the Ag NPs. Hence, it is more reasonable to regard Ag–AgCl composite as AgCl semiconductor sensitized by Ag NPs, which could induce two phonons excitation with an enhanced efficiency. The free electrons from the silver NPs, accompanying with those from $BiVO_4$ conduction band, can be scavenged by oxygen and transformed into active $O_2^{-\bullet}$. Simultaneously, the photogenerated holes in the AgCl transfer more readily to the valence band of $BiVO_4$ (reaction 5), but not lead to the formation of high active specie, chlorine atoms (reaction 6, 7). This can be rationalized by that the top of valence band for AgCl is 3.4 eV [38], much higher than that of $BiVO_4$ (ca. 2.1 eV) [39]. However, such migration results in a decreased oxidation power of holes. Moreover, the low conductivity of holes in the n-type hole-accepter $BiVO_4$ further limits the photocatalytic activity. That is why the holes are not the main active species in the reaction with Ag–AgCl/$BiVO_4$, and the enhanced activity was observed by adding $NaHCO_3$.

$$AgNPs + h\nu \rightarrow AgNPs^* \quad (1)$$

$$AgNPs^* \rightarrow AgNPs^+ + e^- \quad (2)$$

$$e^- + O_2 \rightarrow O_2^{-\bullet} \quad (3)$$

$$AgNPs^+ + AgCl \xrightarrow{h\nu} AgNPs + AgCl(h^+) \quad (4)$$

$$AgCl(h^+) + BiVO_4 \rightarrow AgCl + BiVO_4(h^+) \quad (5)$$

$$AgNPs^+ + Cl^- \cdots\cdots AgNPs + Cl^0 \quad (6)$$

$$AgCl(h^+) + Cl^- \cdots\cdots AgCl + Cl^0 \quad (7)$$

4. Conclusions

An efficient visible light responsive photocatalyst Ag–AgCl/$BiVO_4$ was prepared via a facile photolysis and calcination method. The effect of synthetic conditions such as Ag contents, molar ratios of NH_4Cl to Ag, calcination temperatures have been explored. The sample with 4 wt% Ag, Cl/Ag = 2 and calcined at 500 °C achieved more than 90% MO reduction under the visible light irradiation for 120 min. The coupling Ag–AgCl formation process has been discussed. The previously formed Ag nanoclusters can be converted into AgCl and form the Ag–AgCl nanocomposite. A proper component is necessary for a high activity. The presence of $BiVO_4$ in the composite makes holes migrate toward the valence band of $BiVO_4$, so as to make $O_2^{-\bullet}$ into the only main active species in the degradation reaction. Moreover, adding a hole scavenger can further increase the photocatalytic activity.

Acknowledgments

This work is financially supported by National Natural Science Foundation of China (No. 20907031). We also gratefully acknowledge the support in SEM measurements by Mr. Gang Li of the Instrumental Analysis Center of Shanghai Jiao Tong University.

Appendix A. Supplementary data

Supplementary data associated with this article can be found, in the online version, at doi:10.1016/j.molcata.2011.10.025.

References

[1] C. Hu, T. Peng, X. Hu, Y. Nie, X. Zhou, J. Qu, H. He, J. Am. Chem. Soc. 132 (2010) 857–862.
[2] H.J. Lewerenz, C. Heine, K. Skorupska, N. Szabo, T. Hannappel, T. Vo-Dinh, S.A. Campbell, H.W. Klemm, A.G. Munoz, Energy Environ. Sci. 3 (2010) 748–760.
[3] A. Fujishima, X. Zhang, D.A. Tryk, Surf. Sci. Rep. 63 (2008) 515–582.
[4] R. Asahi, T. Morikawa, T. Ohwaki, K. Aoki, Y. Taga, Science 293 (2001) 269–271.
[5] A. Zielinska-Jurek, E. Kowalska, J.W. Sobczak, W. Lisowski, B. Ohtani, A. Zaleska, Appl. Catal. B: Environ. 101 (2011) 504–514.
[6] M.C. Long, W.M. Cai, Visible light responsive TiO_2 modified with nonmetal elements, Front. Chem. China (2011).
[7] X. Chen, S. Shen, L. Guo, S.S. Mao, Chem. Rev. 110 (2010) 6503–6570.
[8] H.J. Zhang, G.H. Chen, D.W. Bahnemann, J. Mater. Chem. 19 (2009) 5089–5121.
[9] H.G. Kim, P.H. Borse, W. Choi, J.S. Lee, Angew. Chem. Int. Ed. 44 (2005) 4585–4589.
[10] M. Zhu, P. Chen, M. Liu, ACS Nano. (2011) 4529–4536.
[11] E. Ozbay, Science 311 (2006) 189–193.
[12] H.Y. Zhu, X. Chen, Z.F. Zheng, X.B. Ke, E. Jaatinen, J.C. Zhao, C. Guo, T.F. Xie, D.J. Wang, Chem. Commun. (2009) 7524–7526.
[13] S.A. Maier, M.L. Brongersma, P.G. Kik, S. Meltzer, A.A.G. Requicha, B.E. Koel, H.A. Atwater, Adv. Mater. 13 (2001) 1501–1505.
[14] K. Kneipp, Y. Wang, H. Kneipp, L.T. Perelman, I. Itzkan, R.R. Dasari, M.S. Feld, Phys. Rev. Lett. 78 (1997) 1667–1670.
[15] H.A. Atwater, A. Polman, Nat. Mater. 9 (2010) 205–213.
[16] Z. Liu, W. Hou, P. Pavaskar, M. Aykol, S.B. Cronin, Nano Lett. 11 (2011) 1111–1116.
[17] P. Wang, B. Huang, X. Qin, X. Zhang, Y. Dai, J. Wei, M.-H. Whangbo, Angew. Chem. Int. Ed. 47 (2008) 7931–7933.
[18] P. Christopher, H. Xin, S. Linic, Nat. Chem. 3 (2011) 467–472.
[19] W.H. Hung, M. Aykol, D. Valley, W. Hou, S.B. Cronin, Nano Lett. 10 (2010) 1314–1318.
[20] M. Ashokkumar, J.L. Marignier, Int. J. Hydrogen Energy 24 (1999) 17–20.
[21] N. Kakuta, N. Goto, H. Ohkita, T. Mizushima, J. Phys. Chem. B 103 (1999) 5917–5919.
[22] P. Wang, B. Huang, X. Zhang, X. Qin, H. Jin, Y. Dai, Z. Wang, J. Wei, J. Zhan, S. Wang, J. Wang, M.H. Whangbo, Chem. Eur. J. 15 (2009) 1821–1824.
[23] P. Wang, B. Huang, X. Qin, X. Zhang, Y. Dai, M.H. Whangbo, Inorg. Chem. 48 (2009) 10697–10702.
[24] P. Wang, B. Huang, Q. Zhang, X. Zhang, X. Qin, Y. Dai, J. Zhan, J. Yu, H. Liu, Z. Lou, Chem. Eur. J. 16 (2010) 10042–10047.
[25] P. Wang, B. Huang, Z. Lou, X. Zhang, X. Qin, Y. Dai, Z. Zheng, X. Wang, Chem. Eur. J. 16 (2010) 538–544.
[26] J. Yu, G. Dai, B. Huang, J. Phys. Chem. C 113 (2009) 16394–16401.
[27] S. Kohtani, S. Makino, A. Kudo, K. Tokumura, Y. Ishigaki, T. Matsunaga, O. Nikaido, K. Hayakawa, R. Nakagaki, Chem. Lett. 31 (2002) 660–661.
[28] S. Kohtani, M. Tomohiro, K. Tokumura, R. Nakagaki, Appl. Catal. B: Environ. 58 (2005) 265–272.
[29] S. Kohtani, J. Hiro, N. Yamamoto, A. Kudo, K. Tokumura, R. Nakagaki, Catal. Commun. 6 (2005) 185–189.
[30] J.A. Dean, Lange's Chemistry Handbook Version 15th Section 9, McGraw-Hill Book Co., New York, 1999.
[31] A. Kudo, K. Omori, H. Kato, J. Am. Chem. Soc. 121 (1999) 11459–11467.
[32] X. Xu, Y. Ni, T. Yin, X. Ge, Q. Ye, Z. Zhang, Prog. Chem. 11 (1999) 239–246.
[33] B. Xie, H. Zhang, P. Cai, R. Qiu, Y. Xiong, Chemosphere 63 (2006) 956–963.
[34] H.P. Boehm, Discuss. Faraday Soc. 52 (1971) 264–275.
[35] K. Sayama, H. Arakawa, J. Chem. Soc., Faraday Trans. 93 (1997) 1647–1654.
[36] Y. Wang, Y. Wang, Y. Gao, React. Kinet. Mech. Catal. 99 (2010) 485–491.
[37] S. Glaus, G. Calzaferri, J. Phys. Chem. B 103 (1999) 5622–5630.
[38] J. Tejeda, N.J. Shevchik, W. Braun, A. Goldmann, M. Cardona, Phys. Rev. B 12 (1975) 1557–1566.
[39] M.C. Long, W.M. Cai, H. Kisch, J. Phys. Chem. C 112 (2008) 548–554.